

Demystifying Integrated Power and Desalination Processes Evaluation based on Standard Primary Energy Approach

Muhammad Wakil Shahzad^{1*}, Kim Choon Ng², Muhammad Burhan², Qian Chen²,
Muhammad Ahmad Jamil¹, Nida Imtiaz¹ and Ben Bin Xu¹

¹Department of Mechanical and Construction Engineering, Northumbria University,
Newcastle Upon Tyne NE1 8ST, United Kingdom.

²Water Desalination and Reuse Centre, King Abdullah University of Science & Technology, 23955-
6900 Thuwal, Kingdom of Saudi Arabia.

*muhammad.w.shahzad@northumbria.ac.uk

Abstract

The energy efficiency of seawater desalination processes is usually expressed in terms of kWh electricity or low-grade heat per cubic meter of water produced. This energy efficiency evaluation criteria unfortunately omitted the embedded quality of derived energy input. To have fair comparison of assorted desalination processes, it is important to consider quantity as well as quality of derived energy input based on their generation mechanisms. The numerator (m^3 of distillate produced) and denominator ($\text{kWh}_{\text{derived energy}}$ consumption) terms in energy efficiency evaluation are to be benchmark onto a common platform for fair evaluation and comparison. An inadequate comparison may result in an inferior adaptation of desalination methods that can lead to high economical destruction. In this article, a detailed thermodynamic framework has been developed to convert cogeneration-based electricity and heat into standard primary energy input. The proposed standard primary energy platform will help to demystify the quality and quantity aspects of derived energy supply. The thermodynamic based rigorous calculations show that 1.813 units of primary energy are required to produce one unit of electricity due to conversion efficiencies and losses involved in the power plant. On the other hand, one unit low-pressure steam to operate thermally driven desalination cycles need only 0.0944 units of primary energy. This stark difference clearly shows that omitting the grade of energy in performance evaluation can lead to an in-efficient installation decision. This proposed framework will provide a basic ground for future efficient processes selection and assorted processes evaluation at common platform.

Keywords: Standard primary energy, processes comparison, conversion factor, sustainable desalination, Thermodynamic limit.

1. Introduction

Global water demand continues to grow at a CAGR rates of 7-8% whilst the sources of freshwater are becoming more scarce due to over withdrawn of ground water in many water-stressed regions [1]. The major factors of increasing the water demand are, industrialization, agriculture cultivation for higher food needs of population growth and change in lifestyle. The urbanization and better lifestyle have unknowingly imposed a huge impact on water demand due to increasing consumption and packaging of food. For example, the current fast and processed food need much water in preparation for consumption as compared to simple food availability in the farms. The average water footprint, expressed in litres of water per item, for a host of common food items that we took for granted are shown in Figure 1 [2].



















	1 tomato 13 litres		1 potato 25 litres		1 cup of tea 35 litres
	1 bread slice 40 litres		1 egg 135 litres		1 cup of coffee 140 litres
	1 wine glass 120 litres		1 beer glass 75 litres		1 glass apple juice 190 litres
	1 kg wheat 1300 litres		1 kg corn 900 litres		1 kg soyabean 1800 litres
	1 kg chicken 2900 litres		1 kg pork 4800 litres		1 kg beef 15500 litres
	1 hamburger 2400 litres		1 kg chocolate 24000 litres		1 cup of milk 200 litres

Figure 1: A summary of water footprint of food items for our daily consumption [2].

As per UN report, today, 4.2 billion (55%) population live in urban areas and it is expected to increase to 68% by 2050, more than doubling its current size, nearly 7 of 10 people in the world will live in cities [3]. The urbanization trend in 21st century is most significant, and it has severe impact on energy consumption and food-water nexus management. It is projected that global water withdrawal will surge up to 4,500 billion cubic meter (bcm) by 2040 and water consumption is predicted to increase up to 1750 bcm [4]. The water demand for energy production and agricultural sectors are also growing exponentially due to higher population growth and relentless quest for oil & gas exploration [5]. Interestingly, water consumption for power generation sector has a slight reverse trend since 2014, due primarily to wider application of renewable energy resources [6]. On the other hand, water consumption in the agriculture sector is deemed as the highest at 75 % of overall consumption in the next two decades as it is estimated that agricultural production will need to expand by approximately 70% by 2050 [7]. Water consumption distribution for all sectors from 2014-2040 is presented in Figure 2 [8].

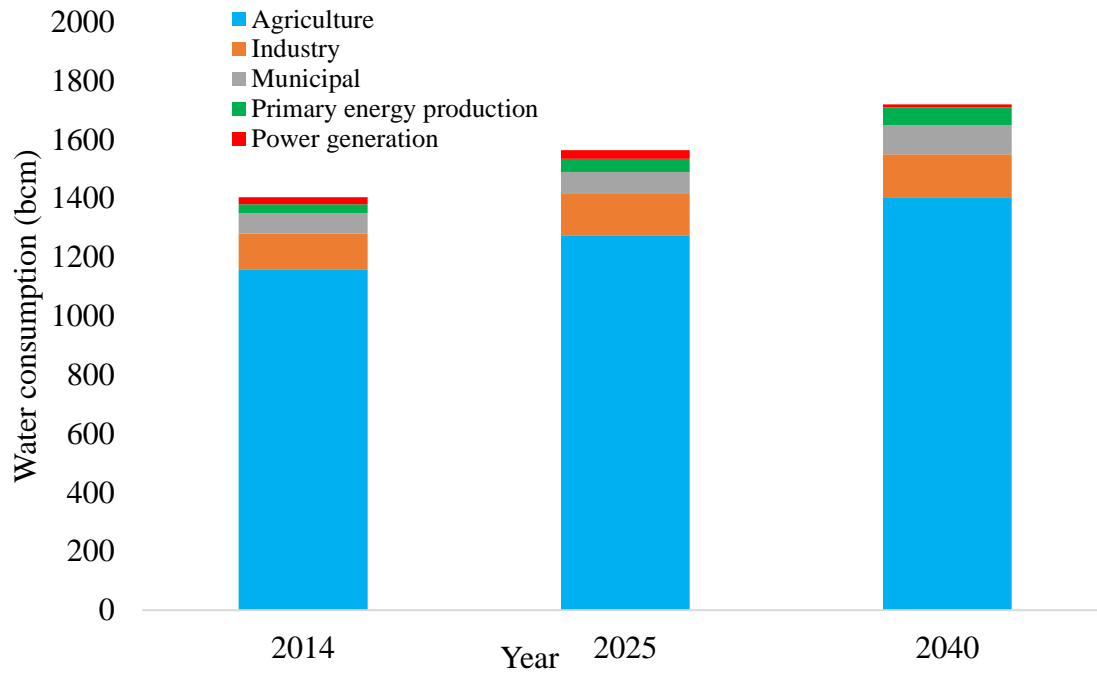


Figure 2: Water consumption by different sectors from 2014-2040 [8].

Presently, 1.2 billion people live in physical scarcity regions and additional 600 million people are approaching this situation. With the existing climate change scenario, almost half the world's population is expected to live in high water stress regions by 2030, including 250 million people in Africa [9]. BBC reported that 11 cities are marked as red and most likely to run out of drinking water by 2050 are São Paulo, Bangalore, Beijing, Cairo, Jakarta, Moscow, Istanbul, Mexico City, London, Tokyo and Miami. Many of countries depended on ground and surface water to fulfil their demand but in arid region these natural sources availability has diminished significantly, as shown in Figure 3 [10]. Reports shows that the conventional water sources such as aquifers, rivers, lakes, snowmelts and rainfall are not sufficient to meet the minimum water requirements per capita in the water stress countries. The United Nation Sustainable Development Goal (SDG) 6 aim to provide clean water for present and future generation but current situation is directly conflicting with the expected targets.

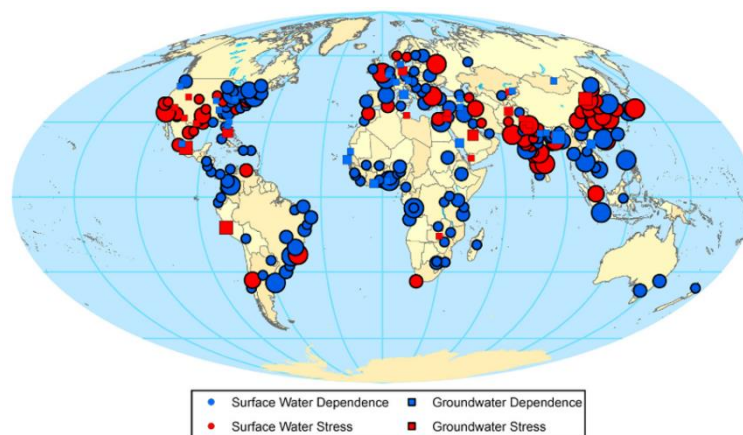


Figure 3: Surface and ground water dependence and stress region around the world [10].

The water stress countries have to re-think radically for water resources planning for their future sustainable water supplies. The most accepted and practically viable solutions are seawater and brackish water desalination processes [11].

2. Separation Processes

Seawater desalination processes has been around for centuries and over time they become more sophisticated. As per IDA Desalination Yearbook 2018-2019 report, over 18,000 desalination plants in 150 countries are producing 100 million cubic meter (mcm) water per day to supply 300 million peoples as shown in Figure 4 [12]. In terms of installed capacities, 48% is installed in Middle East and North Africa (MENA) region, followed by East Asia and Pacific 18.4%, North America 11.9%, China 7.5% and US 11.2% [12].

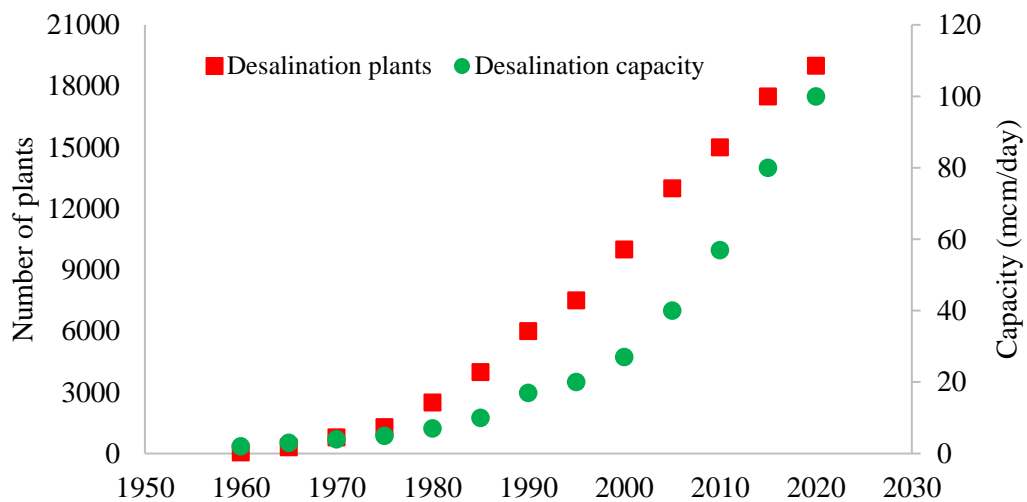


Figure 4: Global desalination capacity and number of plants [12].

Desalination processes can be applied to seawater and other nonpure water sources. Presently, 61% fresh water is produced from seawater desalination processes followed by 21% from Brackish water and 8% from River water. Overall, 90% of fresh water is produced from these three sources and remaining is extracted from wastewater, brine and other sources as shown in is Figure 5 [13].

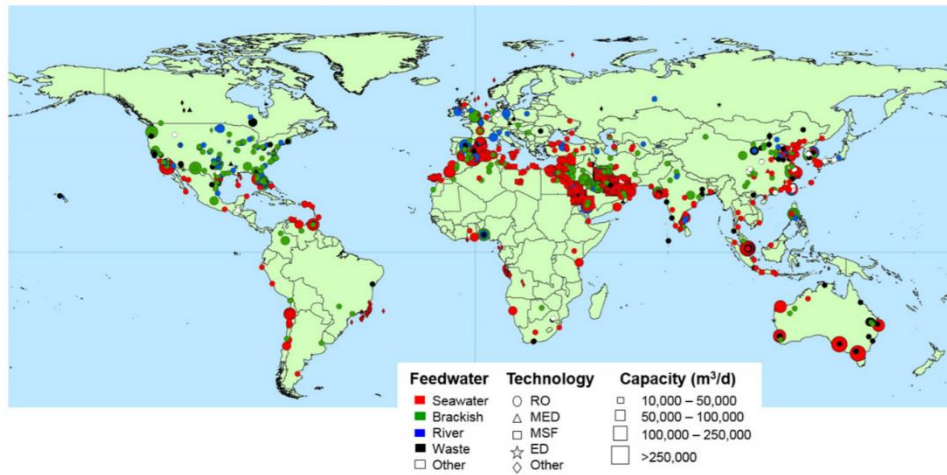


Figure 5: Desalination processes based on feed water at different part of the world [13].

Separation of additional salt from seawater involve substantial amount of energy that makes them not only energy intensive but also environmental unfriendly due to CO₂ emissions and excessive chemicals discharge [14–16]. The theoretical lowest separation energy of seawater of concentration 35000 mg/L and temperature of 28°C is around 0.78 kWh/m³ [17,18]. Unfortunately, all practical desalination technologies, such as multi effect desalination (MED) [19–26], multi stage flash (MSF) [27–29] and Seawater reverse osmosis (SWRO) [30,31] are operating at 8-10 times higher than theoretical minimum energy requirement or thermodynamic limit (TL). Almost 95% online desalination capacity is based on these three major but practical processes. Within these three processes, two major categories such as thermally driven MED & MSF and pressure driven SWRO application depend on seawater quality, electricity and steam requirements and footprint. The amount of chemicals required in pre-treatment of seawater feed also varies with type of desalination processes that may have a detrimental effect to marine life. There were many other new technologies proposed claiming high performance but unfortunately none of them succeeded to reach a commercialization state [32]. Thus, the conventional processes such as MED, MSF and SWRO are still considered reliable and secure to provide drinking water in water stress countries.

In general, desalination processes can be designed as a standalone or collocated with power plant. One of the lessons learned from history is, the co-location of power plants and desalination processes can **achieve** maximum utilization of primary fuels in terms of having greater thermodynamic synergy, particularly the integration of assorted types of thermal desalination processes with the electricity generation plant. In addition to process synergy, in co-location arrangements, both plants **share** many utilities that reduces individual infrastructure requirements. However, there is no clear framework for energy consumption evaluation of each process in a combined power and water plants. Since power generation and water production utilize different grade of input energy in terms of pressure and temperature so it is very important to embed the quality of working steam supplied during performance evaluation of various process. It is therefore timely and necessary to develop a simple but rigorous thermodynamic methodology to calculate the conversion factors from various grade of derived

or secondary energy to primary energy input. In this article, we **present** the detailed investigation of power plant combined with desalination processes, particularly the calculations of conversion factors for electricity and heat to primary energy supplied to evaluate the apportionment of input energy consumption for useful derived or secondary energy. This simple conversion factors framework based only on operational temperatures is presented for the first time for combined power and desalination plants.

3. Combining Power and Separation Processes

The co-location of power and desalination system is beneficial if both systems have thermodynamic synergy where the processes are cascaded with favourable pressure and temperature drop. For example, combined cycle gas turbine (CCGT) and thermally driven desalination system MED and MSF have excellent synergy in this respect. Their integration maximizes the exergy or work potential from the primary fuel burned [33]. In a typical combined cycle system, the primary fuel is burned in combustion chamber of gas turbine cycle. High temperature and high-pressure gases are expanded through gas turbine (GT) and **produce** electricity through generator system. The exergy of exhaust gases leaving from GT is further utilized in heat recovery steam generator (HRSG) to produce high pressure and high temperature steam for the bottoming Rankine cycle. The steam, at 562°C and 114 bar, is first passed through high pressure steam turbine (ST-1) to produce electricity. The steam is reheated again in HRSG, to the same temperature but at 26 bar, before introducing into medium pressure turbine (ST-2) to be followed by low pressure steam turbine (ST-3). All steam turbines share common shaft of the electric generator to produce electricity. Only a small fraction of low pressure and temperature steam is bled-off from last stages of low-pressure (LP) turbine to power the thermal desalination cycle such as MED augmented with a thermal vapour compressor (TVC). It is noticed that Rankine cycle is designed to operate all turbines stages with favourable temperature cascade (from ST turbines) and MED-TVC desalination cycle. The latter is powered by bled steam with a top-brine inlet not greater than 65°C and it depicts an excellent thermodynamic synergy in the multiple reuse of the latent heat of condensation at every MED stages. A typical combined CCGT power and desalination plant is shown in **Figure 6 (a, b)**.

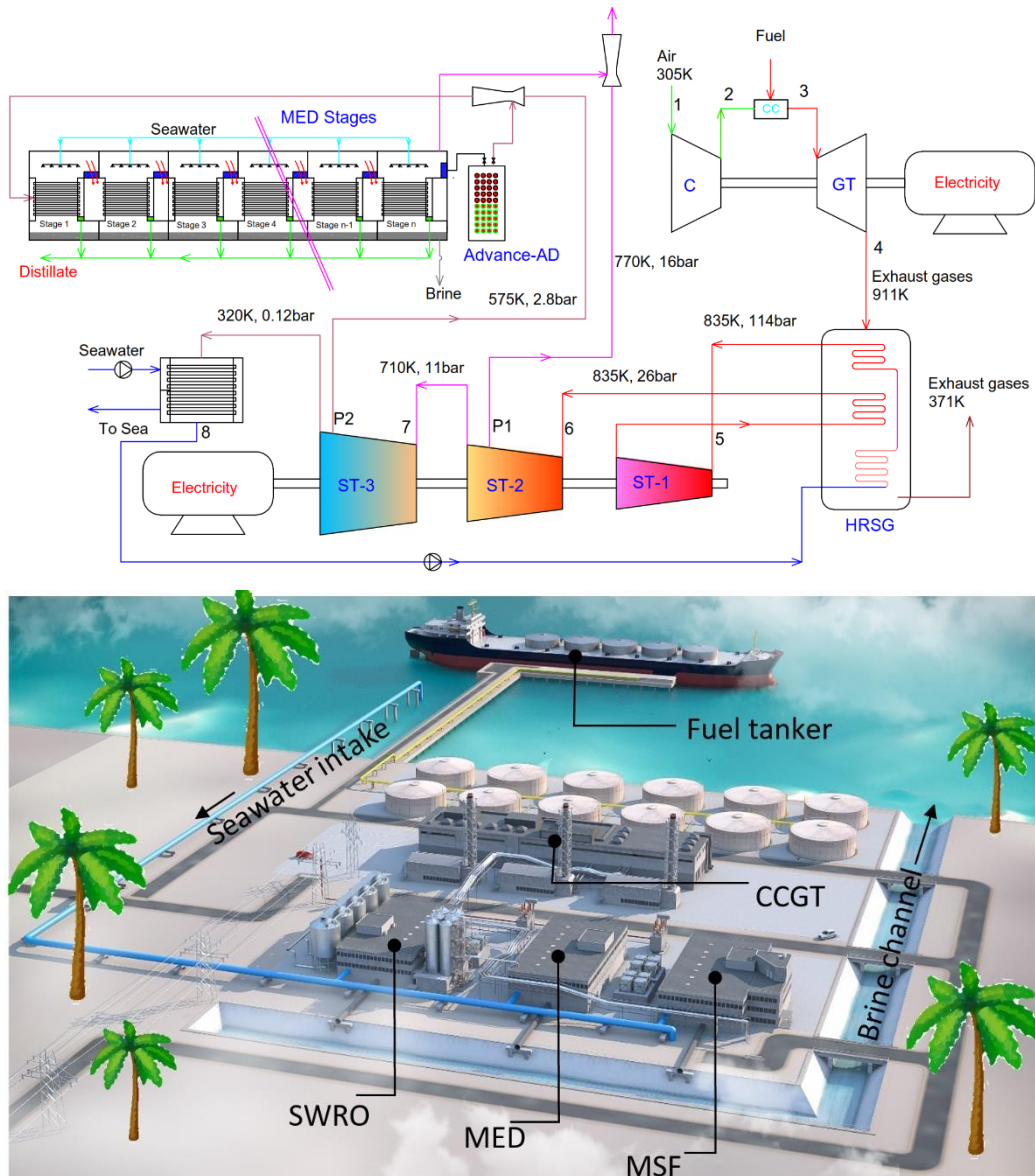


Figure 6: (a) Schematic of combined CCGT and desalination plant, (b) Pictorial view of practical combined power and desalination cycle for electricity and water production.

Today's commercial seawater desalination plants are designed from 10,000 to million m^3/day capacity, consuming derived energy such as electricity and low-grade thermal heat sources, and the figure of merits (FOMs) depicting are expressed usually in the form of kWh_{elec} or kWh_{ther} per cubic meter of water produced [34]. The major issue of using such FOMs is the misconception of the seeming parity of the derived energy consumed, i.e., $1 \text{ kWh}_{\text{elec}}$ is not equal to $1 \text{ kWh}_{\text{ther}}$, underlying the production of derived energy. The need to discern both the quantity and embedded quality of derived energy consumption by desalination methods is the key to have accurate and meaningful energy efficacy analysis across processes. We embedded both quality and quantity of derived energies in proposed thermodynamic framework as presented in following sections.

4. Thermodynamic Framework for Combined Processes Energy Evaluation

From classical thermodynamics, the importance of energy quality at a given unit amount of heat transfer can be demonstrated graphically with three ideal heat engines, operating arbitrary from three levels of heat source (T_H) to ambient ($T_o=303K$) temperatures, namely $T_{H1}= T_{adia}=1750K(1477^\circ C)$, $T_{H2}=750K(477^\circ C)$, and $T_{H3}=333K(60^\circ C)$, as shown in Figures 7. All Carnot cycles assumed to extract a unit heat input (1 kWh) from the higher isotherm (T_H), whilst low-grade heat is rejected at the lower isotherm (T_L). Between these isotherms, two isentropes ($\Delta S=0$) linked their edges to form a cyclic engine [35,36].

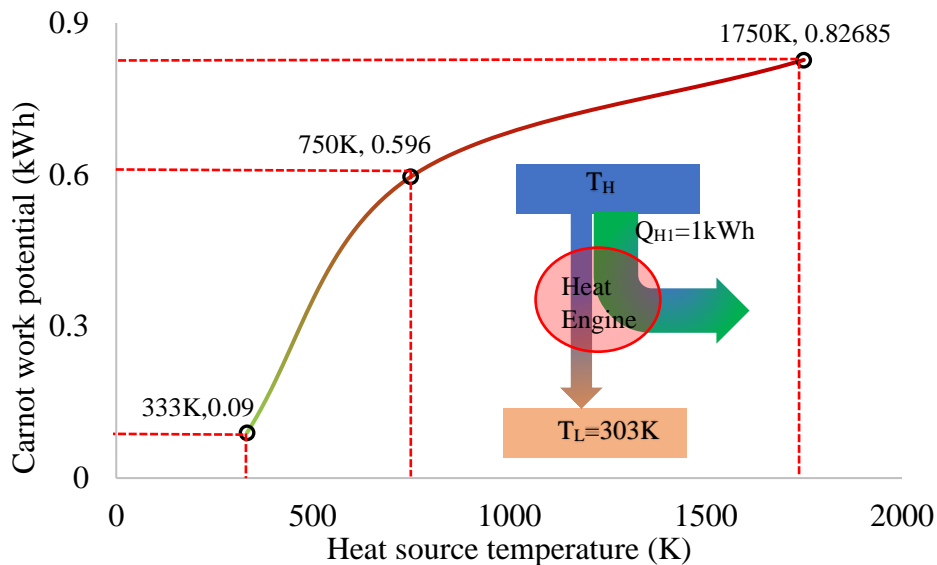


Figure 7: Heat engines operating at assorted heat input (but with 1kWh heat input) and their respective Carnot work potential.

With these assumptions, the heat engines are deemed internally and externally reversible, i.e., zero entropy generation during heat transfers. By adopting an ideal heat engine framework of power plants, two causal relations or corollaries can be expounded *vis-à-vis* underlying derived energy production methods: Firstly, the exergy of input fuel to a power plant can be apportioned accurately with respect to its Carnot work production. Each temperature-cascaded cycle or device operates within the designed high and low-temperature reservoirs, producing the needed derived energy for external use. Secondly, only the Carnot work generated from the array of heat engines could be “decomposed” respectively to a primary energy platform, as depicted schematically in Figure 8. In this framework, only the equivalent primary energy, defined at the adiabatic flame to the ambient temperature, is thermodynamically meaningful for direct comparison between desalination processes consuming assorted types of derived energy, for example, electricity and low-grade heat driven processes. Figure 8 shows a typical commercial-scale CCGT integrated with MED-TVC for seawater desalination, consuming natural gas and produce electricity and water.

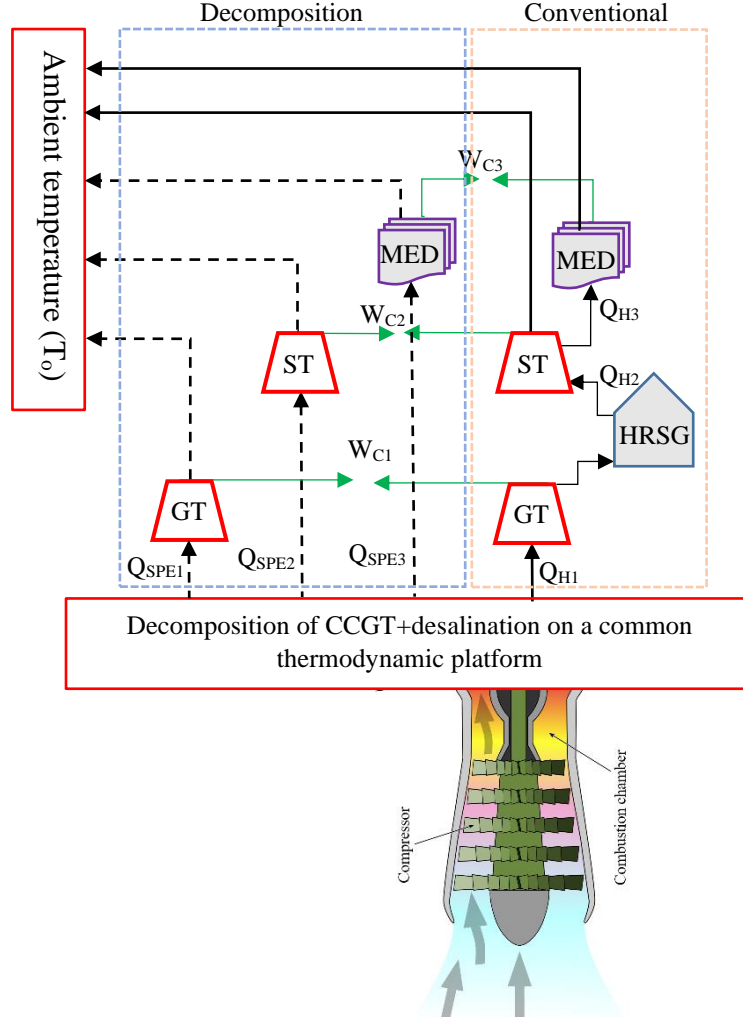


Figure 8: CCGT power and desalination plant and its decomposition to the SPE platform.

5. Conversion Factors Calculation

In a simple heat engine or reversed engine, one of the corollaries that can be formulated from the application of 1st and 2nd Laws of Thermodynamics is given as:

$$\frac{W_C}{(T_H - T_L)} = \frac{Q_H}{T_H} = \frac{Q_L}{T_L} \quad (1)$$

where the symbols used have their usual meanings, as depicted by Figure 7. For a heat engine, the causal relation between heat and work transfers is expressed as

$$W_C = Q_H \left(1 - \frac{T_L}{T_H} \right) \quad (2)$$

whilst in a reversed engine (like a chiller or refrigerator), a similar relation is expressed as

$$-W_C = -Q_L \left(\frac{T_H}{T_L} - 1 \right) \quad (3)$$

The minus sign indicates heat is extracted from the reservoir or work is input to the Carnot or ideal reversed cycle. For seawater desalination applications, we select a thermally-driven MED-TVC for the production of potable water. The primary fossil fuels, such as natural gas, liquid fuels, etc., are usually burned in combustor of gas turbines to operate a series of conversion or separation processes. Through these temperature-cascaded ideal cycles, assorted forms of derived energy are produced and conveniently supplied for external use. In recent decades, the best power plants available hitherto is the combined cycle gas & steam turbines or simply known as the CCGTs. It is essential that the underlying processes incurred in the production of derived energy are evaluated by the apportionment of total primary energy input from fuels. Logically, only the most efficient power plants are employed in the thermodynamic framework, and it presents the least primary energy needed for derived energy production. Between the ideal output of heat engines and the actual production or consumption of derived energy in real processes, the first and second law efficiencies (η , η'') of respective cycles are exploited for calibration to yield the conversion factors (CF) for respective derived energy type, i.e., $CF_{elec.}$ and $CF_{ther.}$. These CFs could transform the derived energy consumption to a primary energy platform.

As the derived energies were conveniently supplied to all types of desalination processes by operation, the seeming parity assumption between electricity and low-grade heat has led to the thermodynamic misconception in a direct comparison of their energy efficacy. Presently, all derived energies used are by expressed by kWh (3.6 MJ). Yet underlying the derived energy generation at the power plants, i.e., it is evident from the distribution of primary energy consumption in producing 1 kWh electricity is not equal to 1 kWh of low-grade heat. Despite similar quantitative units of measurement, the unwarranted methodology is traced to the ignorance of embedded energy quality that accompanied in the supply of a type of derived energy. This obvious fallacy has been perpetuated, unintentionally, for decades in all industrial processes, such as in desalination, cooling, as seen by the voluminous literature. In this paper, we addressed the absolute value of derived energy in one application, namely the consumption of derived energy by the seawater desalination methods. The primary energy defined by the available work of fossil fuel burned at its adiabatic flame (in air) temperature (T_{adia}) with respect to the low temperature reservoir, i.e., ambient state (T_o). Thus, the apportionment of primary energy input by thermodynamic framework forms the energy standards that accounted for both quantitative and qualitative aspects of derived energy consumption. This novel primary energy platform is then utilized for the comparison of energy efficacy of all desalination methods.

Invoking Eq.(1) for a cyclic heat engine operating across the designed temperature reservoirs, the Carnot work is simply given by Eq. (4). As the Carnot work has embedded quantitative and qualitative aspects of energy supply (Q_H) to heat engines, it could be transformed to any common energy platform. In this paper, we **propose** a highest exergy platform that is defined by the adiabatic flame and ambient temperatures, and it is termed as the “standard primary energy (SPE)” platform, i.e.,

$$\overbrace{Q_H \left(1 - \frac{T_L}{T_H}\right)}^{\text{Designed cycle at temperature reservoirs } T_L \text{ and } T_H} = W_C = \overbrace{Q_{SPE} \left(1 - \frac{T_o}{T_{adia}}\right)}^{\text{Common primary energy platform } (T_{adia}, T_o) \text{ to give same } W_c.} \quad (4)$$

For relevance to actual processes, we invoked the 2nd Law efficiency to relate the actual to Carnot work, i.e., $W_a = \eta'' W_C$. Substituting for the W_C of Eq. (4), we obtained the ratio of standard primary energy (Q_{SPE}) to the actual work (W_a) via the 2nd Law efficiency and the temperature ratio based on the T_o and T_{adia} . Hence the conversion factor for any electrically-driven systems, where the majority of electricity supply were produced by CCGTs, can be expressed as

$$CF_{elect.} = \left(\frac{Q_{SPE}}{W_a}\right) = \frac{1}{\eta'' \left(1 - \frac{T_o}{T_{adia}}\right)} \quad (5)$$

In a heat-driven plant, a similar causal expression can be formulated. By invoking the 1st and 2nd Law efficiencies of any process, the heat supply (Q_a) is predicated at the designed temperature reservoirs, i.e., $\eta Q_a = W_a = \eta'' W_C$. Hence, the ratio of these efficiencies is simply defined by the ratio of Carnot work to the measured heat rates of the plant, that is $\frac{\eta}{\eta''} = \frac{W_C}{Q_a}$. For a thermally-driven cycle consuming a Q_a heat rate, its equivalent Q_{SPE} is deduced to the conversion factor, CF_{ther} , i.e.,

$$CF_{ther.} = \left(\frac{Q_{SPE}}{Q_a}\right) = \frac{\eta}{\eta''} \frac{1}{\left(1 - \frac{T_o}{T_{adia}}\right)} \quad (6)$$

An unique thermodynamic feature of Eq.(5) and (6) is that they could be pre-calibrated in a best available type of power plants underlying the production of the assorted types of derived energy consumed by the desalination plants, namely electricity for SWRO and low-temperature heat sources for MSF and MED. By applying these CFs, the known specific derived energy efficiency of all existing desalination plants, namely expressed either in $\text{kWh}_{elec}/\text{m}^3$ or $\text{kWh}_{ther}/\text{m}^3$, could be transformed to the common platform of standard primary energy, i.e., Q_{SPE}/m^3 . We employed the temperature-cascaded cycles and the nominal heat rates from the combustion of natural gas in a typical CCGT to calibrate the CFs for electricity and heat supply of practical desalination plants.

6. Calibration of Conversion Factors

For the typical CCGT power plants available today, the computed conversion factors of electricity (CF_{elect}) and low-grade heat at 110°C (CF_{ther}) input are found to be 1.811 and 0.094 respectively. Alternatively, one could infer from the thermodynamic framework that the consumption of 1 kWh_{elec} is $1.811/0.094 = 19.2$ times more valuable than 1 $\text{kWh}_{thermal}$ of low-grade heat (steam at 373K). Note that the denominator of both factors are expressed in terms of the actual quantitative consumption of derived energies, i.e., W_a or Q_a measured at their designed states. The transformation to equivalent Q_{SPE} has embedded its corresponding energy quality through specifying the 1st and 2nd law efficiencies of respective processes. For the

electricity production from gas and steam turbines, the weighted 2nd law efficiency (η'') is computed as 66.7%, whilst for the thermally driven TVC-MED distillation, the ratio of 1st (η) to 2nd (η'') law efficiencies, (η / η'') is 0.0781. The detail of CFs calibration is presented in Table 1.

Table 1: Conversion factors calibration

Major types of equipment used for derived energy production of CCGT ($Q_{input}/Q_{SPE}=1.0$) Nominal $Q_{input}=2000$ MW.	Designed temperature reservoirs.		Equivalent Q_{SPE} $Q_{SPE} = \frac{W_C}{(1 - \frac{T_o}{T_{adia}})}$	1st Law Efficiency ($\eta = \frac{W_a}{Q_H}$), and 2nd Law Efficiency ($\eta'' = \frac{W_a}{W_C}$)	Conversion factor (CF)
	T_H (K) / T_L (K)	Carnot work (W_C)			
Gas Turbines (GT) $W_a = 768.87$ MW	1750 / 911	0.4794	0.5798	$\eta = \frac{W_a}{Q_H} = \frac{768.87}{2000} = 0.3844$ $\eta'' = \frac{W_a}{W_C} = \frac{(768.87)}{0.4794} = 0.8018$	$CF_{elec,GT} = \frac{Q_{SPE}}{W_a} = \frac{1}{(0.8018)(0.82685)} = 1.508$
Heat recovery steam generator HRSG (air side)	911/303	(0.3474)	0.4202	-/-	-
Summation (W_C & Q_{SPE})	-/-	0.8269	1.0	-/-	-
Steam Turbines stages (ST), $Q_{H,ST}/Q_{input}=0.5205$ $W_{a,ST} = 325.5$ MW	T_H (K) / T_L (K)	W_C	Q_{SPE}	1 st and 2 nd Law efficiencies	CF
ST-1	911 / 653	0.1217	0.1472	Weighted efficiencies: $\eta'' = \frac{\sum(W_{a,ST})}{\sum(Q_{SPE,ST})} = 0.4773$	$CF_{elec,ST} = \frac{Q_{SPE}}{Q_a} = \frac{1}{(0.4773*0.82685)} = 2.533$
ST-2	911 / 560	0.1349	0.1632		
ST-3	560 / 303	0.08426	0.1019		
Weighted conversion factor, CF_{elec} , for Gas and Steam Turbines.	-			Weighted by GT and ST, $(\eta'')_w = 0.667$	$CF_{elec} = \frac{1}{(0.82685*0.667)} = 1.813$
Bled steam (@100°C) driven Thermal vapor compressor (TVC) and Multi-effect distillation plant (MED)	373 / 315	(0.00928)	0.01122	$\frac{\eta}{\eta''} = \frac{W_C}{Q_a} = 0.0781$	$CF_{thermal} = \frac{Q_{SPE}}{Q_a} = \frac{1}{\eta''(1 - \frac{T_o}{T_{adia}})} = \frac{0.0781}{(0.82685)} = 0.0944$
Summation of all Q_{SPE}	-	-	≈ 1.0	Ratio of $(Q_{elec}/Q_{ther})_{SPE}$	$= 1.811/0.0944 = 19.18$

The earlier presented CFs [37–40] are complicated and need more operational information for conversion of derived energies into primary energy. From Table 1, it can be seen clearly that the proposed CFs only need operational temperatures to convert derived energies into SPE.

7. Conversion Factors Application for Separation Processes Evaluation

Over 40 commercial-scale seawater desalination plants operational data have been collected to evaluate their performance based on proposed standard primary energy platform [37]. Figure 9 depicts the energy efficacy expressed in the tradition format of useful output (m^3 of potable water production) to energy input but the denominator entailed the standard primary energy (Q_{SPE}), i.e., $\text{m}^3/\text{kWh}_{\text{SPE}}$. Thermodynamically, such a figure of merit (FOM) could be compared with an ideal energy efficacy at the thermodynamic limit (TL) of a seawater desalination. At the TL, the FOM is found to be $1.06 \text{ m}^3/\text{kWh}_{\text{SPE}}$, which is equivalent to $W_C=0.78 \text{ kWh}/\text{m}^3$ (seawater is assumed to have 3.5% salts by weight & 25°C) and Q_{SPE} at the standard primary energy platform is $=0.78/0.82685=0.943 \text{ kWh}_{\text{SPE}}/\text{m}^3$). It is noted that the SWRO tends to have a slightly higher water production per unit kWh_{SPE} , due to higher permeate rates at higher trans-membrane pressures (TMP) as compared to the handling of vapor from distillation or flashing method. However, the distillate obtained from the MED and MSF processes is contamination free due to the Angstrom-sized (10^{-10}) molecules of generated vapor. However, recent pilot tests with hybrid thermally-driven processes, namely the integration of adsorption cycles with the MED stages [22,41–46] has boosted higher water performance ratio up to 20% of TL, $0.21 \text{ m}^3/\text{kWh}_{\text{SPE}}$.

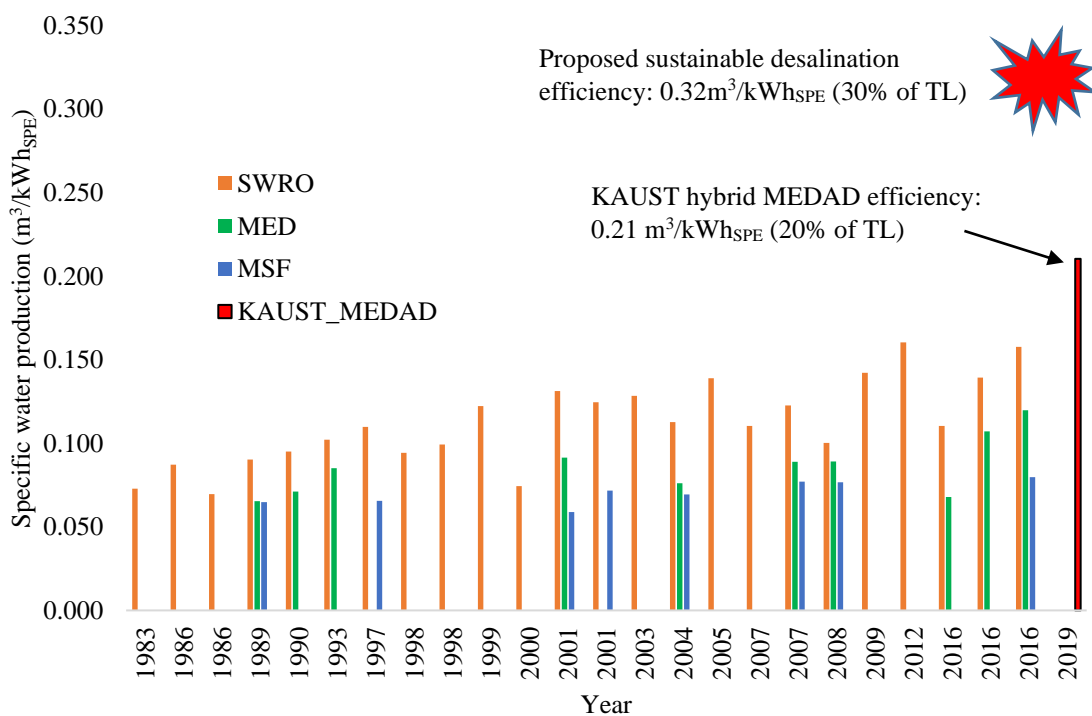


Figure 9. Desalination performance at proposed SPE platform.

8. Conclusion

A thermodynamic framework has been developed and demonstrated, providing the key causal conversion factors for capturing both quantitative and qualitative aspects of the derived energy consumed by assorted desalination methods. These conversion factors, namely CF_{elec} (electricity) and CF_{ther} (low-grade heat source at assorted supply temperatures), were formulated thermodynamically underlying their generation amongst superior power plants available hitherto. Further to their rigorous platforms in converting specific efficiency data to the common standard primary energy (Q_{SPE}) needed in efficacy comparison, the framework has defunct the seeming parity misconception of electricity and low-grade heat, i.e., 1 kWh_{elec} is proven not equal to 1 kWh_{ther} . Such an unfortunate thermodynamic fallacy has deluded all professionals and owners of desalination and other industries alike for decades, particularly the pedagogical needs of a common standard energy platform when comparing energy efficiency amongst all practical heat engines.

Acknowledgement

Authors would like to thank Northumbria University, Newcastle Upon Tyne NE1 8ST, United Kingdom and King Abdullah University of Science and Technology, Saudi Arabia for the research support of this research.

Abbreviations

CAGR	Compound Annual Growth Rate
SDG	Sustainable Development Goals
IDA	International Desalination Association
MENA	Middle East and North Africa
MED	Multi Effect Desalination
TVC	Thermal Vapor Compressor
MSF	Multi Stage Flash
SWRO	Seawater Reverse Osmosis
CCGT	Combined Cycle Gas Turbine
GT	Gas Turbine
HRSG	Heat Recovery Steam Generator
ST	Steam Turbine
SPE	Standard Primary Energy
CF	Conversion Factor
FOM	Figure of merit

References

- [1] Boretti A, Rosa L. Reassessing the projections of the World Water Development Report. *Npj Clean Water* 2019;2. <https://doi.org/10.1038/s41545-019-0039-9>.
- [2] Figueroa AJ. Water footprint of food n.d. <https://jwafs.mit.edu/news/2018/j-wafs-newsletter-highlight-how-much-water-did-you-eat-today> (accessed August 1, 2021).
- [3] Revision W urbanization prospects: T 2018. *World Urbanization Prospects*. vol. 12. Department of Economic and Social Affairs, United Nations; 2018.
- [4] Shahzad MW, Burhan M, Ang L, Ng KC. Energy-water-environment nexus underpinning future desalination sustainability. *Desalination* 2017;413. <https://doi.org/10.1016/j.desal.2017.03.009>.
- [5] Holland RA, Scott KA, Flörke M, Brown G, Ewers RM, Farmer E, et al. Global impacts of energy demand on the freshwater resources of nations. *Proc Natl Acad Sci U S A* 2015;112:E6707–16. <https://doi.org/10.1073/pnas.1507701112>.
- [6] IRENA. IRENA’s Global Renewable Energy Roadmap, REmap 2030: Summary of findings 2014:6.
- [7] Food and Agriculture Organization of the United Nations. *Water for Sustainable Food and Agriculture*. Food and Agriculture Organization of the United Nations; 2017.
- [8] Tiseo I. Projected water consumption from 2014 to 2040 n.d. <https://www.statista.com/statistics/1012228/global-consumption-for-water-by-sector/>.
- [9] Lisa Guppy; kelsey Anderson; Mehta; P.; Nagabhatla; N. and, M. Q. *Global Water Crisis : the Facts* 2017:1–3.
- [10] McDonald RI, Weber K, Padowski J, Flörke M, Schneider C, Green PA, et al. Water on an urban planet: Urbanization and the reach of urban water infrastructure. *Glob Environ Chang* 2014;27:96–105. <https://doi.org/10.1016/j.gloenvcha.2014.04.022>.
- [11] Pistocchi A, Bleninger T, Breyer C, Caldera U, Dorati C, Ganora D, et al. Can seawater desalination be a win-win fix to our water cycle? *Water Res* 2020;182. <https://doi.org/10.1016/j.watres.2020.115906>.
- [12] Association ID. *Water Security Handbook*. vol. 112. 2020.
- [13] Jones E, Qadir M, van Vliet MTH, Smakhtin V, Kang S mu. The state of desalination and brine production: A global outlook. *Sci Total Environ* 2019;657:1343–56. <https://doi.org/10.1016/j.scitotenv.2018.12.076>.
- [14] Tal A. Addressing desalination’s carbon footprint: The Israeli experience. *Water (Switzerland)* 2018;10. <https://doi.org/10.3390/w10020197>.
- [15] Ihsanullah I, Atieh MA, Sajid M, Nazal MK. Desalination and environment: A critical analysis of impacts, mitigation strategies, and greener desalination technologies. *Sci Total Environ* 2021;780:146585. <https://doi.org/10.1016/j.scitotenv.2021.146585>.
- [16] Jia X, Klemeš JJ, Varbanov PS, Alwi SRW. Analyzing the energy consumption, GHG emission, and cost of seawater desalination in China. *Energies* 2019;12:1–16. <https://doi.org/10.3390/en12030463>.
- [17] Ham F van der. Eutectic Freeze Crystallization. Technische Universiteit Delft, n.d.
- [18] Mistry KH, Lienhard JH. Generalized least energy of separation for desalination and other chemical separation processes. *Entropy* 2013;15:2046–80. <https://doi.org/10.3390/e15062046>.
- [19] El-Nashar AM, Qamhiyeh AA. Simulation of the steady-state operation of a multi-effect stack seawater distillation plant. *Desalination* 1995;101:231–43. [https://doi.org/10.1016/0011-9164\(95\)00026-X](https://doi.org/10.1016/0011-9164(95)00026-X).
- [20] Al-Hotmani OMA, Al-Obaidi MAA, John YM, Patel R, Mujtaba IM. Scope and limitations of the mathematical models developed for the forward feed multi-effect

- distillation process-a review. *Processes* 2020;8:1–32. <https://doi.org/10.3390/PR8091174>.
- [21] Eshoul N, Almutairi A, Lamidi R, Alhajeri H, Alenezi A. Energetic, exergetic, and economic analysis of MED-TVC Water desalination plant with and without preheating. *Water (Switzerland)* 2018;10. <https://doi.org/10.3390/w10030305>.
- [22] Hamed OA. Overview of hybrid desalination systems - Current status and future prospects. *Desalination* 2005;186:207–14. <https://doi.org/10.1016/j.desal.2005.03.095>.
- [23] Jamil MA, Goraya TS, Ng KC, Zubair SM, Bin B, Shahzad MW. Optimizing the energy recovery section in thermal desalination systems for improved thermodynamic , economic , and environmental performance. *Int Commun Heat Mass Transf* 2021;124:105244. <https://doi.org/10.1016/j.icheatmasstransfer.2021.105244>.
- [24] Jamil MA, Shahzad MW, Zubair SM. A comprehensive framework for thermo-economic analysis of desalination systems. *Energy Convers Manag* 2020;222:113188. <https://doi.org/10.1016/j.enconman.2020.113188>.
- [25] Jamil MA, Zubair SM. Effect of feed flow arrangement and number of evaporators on the performance of multi-effect mechanical vapor compression desalination systems. *Desalination* 2018;429:76–87.
- [26] Jamil MA, Zubair SM. Design and analysis of a forward feed multi-effect mechanical vapor compression desalination system: An exergo-economic approach. *Energy* 2017;140:1107–20.
- [27] Gao H, Jiang A, Huang Q, Xia Y, Gao F, Wang J. Mode-based analysis and optimal operation of msf desalination system. *Processes* 2020;8. <https://doi.org/10.3390/pr8070794>.
- [28] Toth AJ. Modelling and optimisation of multi-stage flash distillation and reverse osmosis for desalination of saline process wastewater sources. *Membranes (Basel)* 2020;10:1–18. <https://doi.org/10.3390/membranes10100265>.
- [29] El-Ghonemy AMK. Performance test of a sea water multi-stage flash distillation plant: Case study. *Alexandria Eng J* 2018;57:2401–13. <https://doi.org/10.1016/j.aej.2017.08.019>.
- [30] Jamaly S, Darwish NN, Ahmed I, Hasan SW. A short review on reverse osmosis pretreatment technologies. *Desalination* 2014;354:30–8. <https://doi.org/10.1016/j.desal.2014.09.017>.
- [31] Lim YJ, Goh K, Kurihara M, Wang R. Seawater desalination by reverse osmosis: Current development and future challenges in membrane fabrication – A review. *J Memb Sci* 2021;629:119292. <https://doi.org/10.1016/j.memsci.2021.119292>.
- [32] Ahmed FE, Khalil A, Hilal N. Emerging desalination technologies: Current status, challenges and future trends. *Desalination* 2021;517:115183. <https://doi.org/10.1016/j.desal.2021.115183>.
- [33] Wu L, Hu Y, Gao C. Optimum design of cogeneration for power and desalination to satisfy the demand of water and power. *Desalination* 2013;324:111–7. <https://doi.org/10.1016/j.desal.2013.06.006>.
- [34] Ghaffour N, Missimer TM, Amy GL. Technical review and evaluation of the economics of water desalination: Current and future challenges for better water supply sustainability. *Desalination* 2013;309:197–207.
- [35] Caton JA. The thermodynamics of internal combustion engines: Examples of insights. *Inventions* 2018;3. <https://doi.org/10.3390/inventions3020033>.
- [36] Senft JR. *Mechanical Efficiency of Heat Engines*. Cambridge University Press; n.d. <https://doi.org/https://doi.org/10.1017/CBO9780511546105>.
- [37] Ng KC, Burhan M, Chen Q, Ybyraiikul D, Akhtar FH, Kumja M, et al. A thermodynamic platform for evaluating the energy efficiency of combined power

- generation and desalination plants. *Npj Clean Water* 2021;4:1–10. <https://doi.org/10.1038/s41545-021-00114-5>.
- [38] Wakil Shahzad M, Burhan M, Soo Son H, Jin Oh S, Choon Ng K. Desalination processes evaluation at common platform: A universal performance ratio (UPR) method. *Appl Therm Eng* 2018;134:62–7. <https://doi.org/10.1016/j.applthermaleng.2018.01.098>.
- [39] Shahzad MW, Burhan M, Ng KC. A standard primary energy approach for comparing desalination processes. *Npj Clean Water* 2019;2:1–7. <https://doi.org/10.1038/s41545-018-0028-4>.
- [40] Shahzad MW, Burhan M, Ybyraiymkul D, Ng KC. Desalination processes' efficiency and future roadmap. *Entropy* 2019;21. <https://doi.org/10.3390/e21010084>.
- [41] Shahzad MW, Burhan M, Ng KC. Pushing desalination recovery to the maximum limit: Membrane and thermal processes integration. *Desalination* 2017;416. <https://doi.org/10.1016/j.desal.2017.04.024>.
- [42] Ng KC, Thu K, Oh SJ, Ang L, Shahzad MW, Ismail A Bin. Recent developments in thermally-driven seawater desalination: Energy efficiency improvement by hybridization of the MED and AD cycles. *Desalination* 2015;356:255–70. <https://doi.org/10.1016/j.desal.2014.10.025>.
- [43] Ng KC, Thu K, Oh SJ, Ang L, Shahzad MW, Ismail AB. Recent developments in thermally-driven seawater desalination: Energy efficiency improvement by hybridization of the MED and AD cycles. *Desalination* 2015;356. <https://doi.org/10.1016/j.desal.2014.10.025>.
- [44] Shahzad MW, Thu K, Kim Y-D, Ng KC. An experimental investigation on MEDAD hybrid desalination cycle. *Appl Energy* 2015;148. <https://doi.org/10.1016/j.apenergy.2015.03.062>.
- [45] Shahzad MW, Thu K, Saththasivam J, Chun WG, Ng KC. Waste heat operated hybrid (MEDAD) desalination plant: An experimental investigation. *ACRA 2014 - Proc. 7th Asian Conf. Refrig. Air Cond.*, 2014.
- [46] Shahzad MW, Ng KC, Thu K, Saha BB, Chun WG. Multi effect desalination and adsorption desalination (MEDAD): A hybrid desalination method. *Appl Therm Eng* 2014;72. <https://doi.org/10.1016/j.applthermaleng.2014.03.064>.